

## Two regimes of widely tuneable noise-like pulses from a figure-eight fibre laser

This content has been downloaded from IOPscience. Please scroll down to see the full text.

2014 Laser Phys. 24 105104

(<http://iopscience.iop.org/1555-6611/24/10/105104>)

View [the table of contents for this issue](#), or go to the [journal homepage](#) for more

Download details:

IP Address: 130.220.71.24

This content was downloaded on 11/08/2014 at 15:28

Please note that [terms and conditions apply](#).

# Two regimes of widely tuneable noise-like pulses from a figure-eight fibre laser

O Pottiez<sup>1</sup>, B Ibarra-Escamilla<sup>2</sup>, E A Kuzin<sup>2</sup>, J C Hernández-García<sup>2</sup>,  
A González-García<sup>3</sup> and M Durán-Sánchez<sup>4</sup>

<sup>1</sup> Centro de Investigaciones en Óptica (CIO), Loma del Bosque 115, Col. Lomas del Campestre, León, Gto. 37150, Mexico

<sup>2</sup> Instituto Nacional de Astrofísica, Óptica y Electrónica (INAOE), L. E. Erro 1, Sta. Ma. Tonantzintla, Pue. 72824, Mexico

<sup>3</sup> Instituto Tecnológico Superior de Guanajuato, Carretera Guanajuato-Puentecillas km.10.5, Predio El Carmen, Guanajuato, Gto. 36262, Mexico

<sup>4</sup> Mecatrónica, Universidad Tecnológica de Puebla, Ant. Camino a la Resurrección 1002-A Parque Industrial, Puebla, Pue. 72300, Mexico

E-mail: [pottiez@cio.mx](mailto:pottiez@cio.mx)

Received 9 May 2014

Accepted for publication 9 June 2014

Published 1 August 2014

## Abstract

In this paper we study a dispersion-managed figure-eight fibre laser generating noise-like pulses with adjustable characteristics. Non-self-starting mode locking leads to the formation of a single noise-like pulse circulating in the cavity. Both the duration of the pulse and its spectral width can be adjusted by tuning the angle of wave retarders, in particular a half-wave retarder that controls the switching power of the polarization-imbalanced nonlinear optical loop mirror that is used as mode locker. Wave retarder tuning also allows observing an abrupt transition between two clearly distinct noise-like pulse regimes, one characterized by a long ( $> 1$  ns) rectangular pulse envelope with a narrow spectrum and the other characterized by shorter sub-ns bell-shaped pulses whose Raman-enhanced spectrum extends far beyond the doped fibre gain spectrum. The existence of two distinct noise-like pulsing modes can be understood in terms of the periodic variation of the pulse spectrum along the cavity, which is able to shift the effective dispersion regime of the laser. By joining the tuning ranges of each regime, the noise-like pulse duration can be adjusted between 57 ps and 6.3 ns, and its bandwidth between 3.5 and 59 nm.

Keywords: fibre lasers, passive mode locking, noise-like pulses, tuneable lasers

(Some figures may appear in colour only in the online journal)

## 1. Introduction

Because of their ability to produce stable regular trains of optical pulses at a reduced cost, passively mode-locked fibre lasers have been the object of intense research for more than two decades. Although some lasers incorporate semiconductor [1], carbon nanotube-based [2] or graphene-based [3] saturable absorbers (SA), the use of an artificial saturable absorption effect in all-fibre designs, like nonlinear polarization rotation (NPR)-based ring cavities [4] and the so-called figure-eight configuration [5], presents some crucial advantages, like a very fast time response, enhanced flexibility and

higher damage threshold. In the figure-eight cavity design, the SA action is provided by a nonlinear optical loop mirror (NOLM) [6] (or a nonlinear amplifying loop mirror, NALM [7]), and is thus decoupled from the laser cavity, providing superior flexibility and making this architecture particularly attractive.

Although originally aimed at producing intense ultrashort pulses of a few tens of fs [8], the availability of high-power pump diodes and the discovery of new pulsing regimes in strongly normal dispersion cavities [9] are factors that have progressively shifted research interests towards the production of very long, strongly chirped pulses with unprecedented

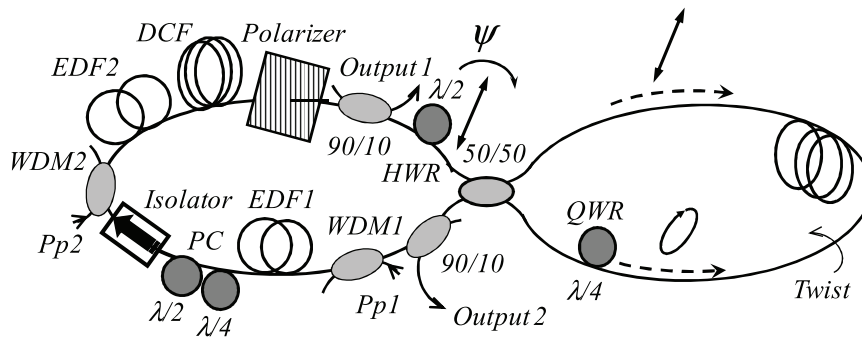


**Figure 1.** Scheme of the figure-eight laser under study.

high energies [3, 10, 11]. Whereas the production of those high-energy pulses is confined in the normal dispersion regime, another category of pulses, the so-called noise-like pulses, were observed recently in both anomalous [12–19] and normal [20–23] dispersion regimes of long fibre lasers. Originally studied in the 1.0 and 1.5  $\mu\text{m}$  wavelength ranges, the noise-like pulsing regime has since been discovered in the 2  $\mu\text{m}$  region as well [24, 25]. Their properties, like high pulse energies [22], wide optical spectrum [18] and short coherence length [12] make those pulses attractive for applications like supercontinuum generation, sensing, etc [26–28]. Basically, a noise-like pulse is a large ( $\sim\text{ns}$ ) and compact collection of thousands of ultrashort (sub-ps) inner pulses, with randomly varying amplitudes and durations. Although their global properties (like the total duration of the bunch, its energy or the average spectrum) remain constant over long periods of time, their inner details (like amplitude and duration of individual sub-pulses) vary widely within each round-trip. As a consequence of their global stability and extreme inner variability, their optical spectrum on average is very smooth. Another typical signature of noise-like pulses is a double-scaled autocorrelation, with a narrow coherence peak riding a wide, smooth pedestal. These two typical features make this regime easily recognizable experimentally.

For several applications, there is an interest in developing noise-like pulse sources with adjustable temporal and spectral characteristics. Several works have shown that, by varying cavity parameters such as its length, dispersion, through pump power or wave plate adjustments, it is possible to tune noise-like pulse properties like their overall duration, coherence peak duration, average peak power and spectral width [13, 14, 17, 22]. In general, such adjustments do not alter the fundamental nature of the noise-like pulsing regime (except, of course, when a transition towards conventional, soliton-like pulsing takes place [13, 15, 16, 20–22, 24, 25]). In fact, the striking uniformity of the experimental data related to noise-like pulsing in the literature (invariably, a wide and smooth spectrum and a double-scaled autocorrelation trace) may lead to the hasty conclusion that noise-like pulsing is one single regime, governed by the same physics without regard to the details of each particular setup. The actual picture is more complex however, and a closer examination of the literature allows discerning several distinct regimes under the general cover of noise-like pulsing operation. For example, in [13],

single- and dual-wavelength noise-like pulses were observed, the latter modality being further subdivided into a coherent and an incoherent mode of operation. In the same reference, long (100s of ps duration) and short (a few ps) noise-like pulse regimes are also distinguished. In [23], single and several multiple noise-like pulsing modes were evidenced. And in [18], two modes of operation can be distinguished, the first one being characterized by a rectangular shape in the time domain and a relatively narrow spectrum, and the other one by a shorter temporal profile and a very wide spectrum.

In this work we study noise-like pulse generation in a passively mode-locked fibre laser. Through simple wave plate adjustments, we are able to tune the temporal and spectral characteristics of the pulses. This work is related to the study performed in [17], with the important difference that the laser cavity is strongly dispersion managed in the present case. We identify two clearly distinct modes of noise-like pulsing, extending very significantly the range of tuneability of the pulses obtained in that reference.

## 2. Experimental setup

The device under study is a figure-eight fibre laser including a ring resonator (figure 1, left) and a NOLM (right side of figure 1). The total cavity length is 189 m. The ring cavity includes 55 m of dispersion-compensating (DCF) fibre ( $D = -38 \text{ ps nm}^{-1} \text{ km}^{-1}$ ) and the NOLM a 100 m loop of low-birefringence fibre ( $D = 17 \text{ ps nm}^{-1} \text{ km}^{-1}$ ). The net cavity dispersion is estimated to  $-0.28 \text{ ps nm}^{-1}$ . The ring also includes two sections of erbium-doped fibre (3 m EDF1 and 2 m EDF2) with  $30 \text{ dB m}^{-1}$  absorption at 1530 nm, which are pumped at 980 nm through WDM couplers. The pump powers into EDF1 and EDF2 are  $P_{p1} = 300 \text{ mW}$  and  $P_{p2} = 200 \text{ mW}$ , respectively. A polarizer ensures linear polarization at the NOLM input, whose angle  $\psi$  can be adjusted by a half wave retarder (HWR). A polarization controller (PC) made of two retarder plates is used to maximize the power through the polarizer. An optical isolator ensures unidirectional laser operation. Two output couplers with 10% output coupling are used as the laser output ports.

Although the NOLM shown in figure 1 is symmetric in power (a 50/50 coupler is used), a polarization imbalance is created by a rotatable quarter-wave retarder (QWR) inserted asymmetrically in the loop [29]. Hence, whereas the clockwise

(CW) beam is linearly polarized, the counter-clockwise (CCW) beam is turned elliptic by the QWR. The two counter-propagating beams thus have different polarization states, and polarization-dependent nonlinear phase shift (or equivalently NPR) constitutes the switching mechanism. Fibre is twisted at a ratio of 5 turns  $\text{m}^{-1}$ , which ensures that the ellipticity of each beam is maintained along the loop [30]. By tuning the orientation of the HWR, the polarization difference between the counter-propagating beams can be adjusted, allowing to tune the NOLM switching power from a minimal value theoretically to infinity [31, 32]. On the other hand, the QWR angle controls the value of low-power transmission, which should be small for pulsed operation in regime, although not zero as some leakage is required to allow lasing to initiate [5].

### 3. Experimental results

At maximum pump power continuous-wave lasing is invariably obtained, however for some adjustments of the wave retarders a slight mechanical stimulation is sufficient to initiate mode locking. The scope trace (figure 2) shows a stable train of pulses with a regular period of 920 ns, and confirms that fundamental mode locking (one single pulse in the cavity) is achieved. The measurement of a smooth optical spectrum and a double-scaled autocorrelation trace reveals the presence of the noise-like pulsing regime. Conventional soliton-like pulse mode locking was never observed. Once mode locking is achieved, the pulse characteristics can be varied through HWR adjustments over some range (figure 3). Beyond this range, however, mode locking is lost and is not recovered through mechanical stimulation unless the HWR is rotated back into the mode locking range.

For a particular HWR angle in the range of mode locking, a sudden transition takes place between two clearly distinct regimes. This transition is reversible: rotating the retarder back and forth about the transition point causes the pulses to switch periodically from one regime to the other. The abruptness of this transition is obvious on the sampling scope, where a several ns long, low-power pulse (figure 3(b)) suddenly turns into a shorter ( $< 1$  ns), high-peak-power pulse (figure 3(a)), or conversely. More precisely, the short pulse is always observed to emerge from the leading (left) edge of the long pulse. Conversely, when the opposite transition occurs, the long pulse systematically grows on the right side of the short pulse. During such transitions, drastic changes are also observed on the autocorrelation trace, especially in terms of signal intensity and pedestal extension, although the variation in the duration of the coherence spur is less significant (figure 3(c)). The transition is also clearly evidenced in the spectral domain, as the spectrum widens or narrows suddenly on the long wavelength side. Besides this abrupt transition, an aspect that fundamentally distinguishes the two regimes is the detail of the pulse features in both temporal and spectral domains. In the long-pulse regime, the pulse envelope displays a flat-topped, nearly rectangular profile (figure 3(b)), whereas intensity varies smoothly with time in the short-pulse regime (figure 3(a)). The long-pulse regime is also characterized by a narrow

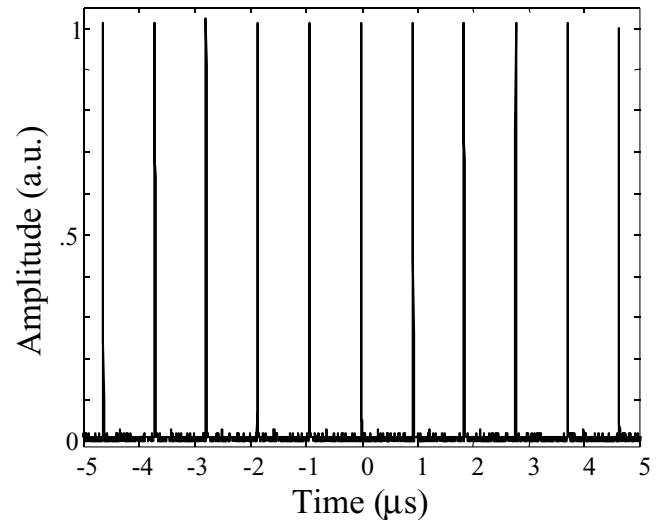


**Figure 2.** Scope trace obtained using a 2 GHz photodetector and a 200 MHz oscilloscope.

spectrum which is nearly symmetric about its maximum, in the 1550 nm region, see figure 3(d) (the secondary peak at 1530 nm is due to spontaneous emission from the doped fibre, which presents a sharp maximum at that wavelength). In contrast, the wide spectrum of the short-pulse regime is strongly asymmetric, with intense components on the long wavelength side that extend up to 1700 nm, shifting the peak wavelength up to 1600 nm. Spectral asymmetry is clearly the signature of Raman self-frequency shift (SFS), which is an important feature of the short-pulse regime due to the higher peak powers that are reached.

By joining the ranges of pulse parameters that are accessible through each of these two regimes, noise-like pulses with a full width at half maximum (FWHM) bandwidth anywhere between 3.5 nm and 59 nm, and with a duration between 57 ps and 6.3 ns, can be obtained through wave retarder adjustments. This corresponds to a factor of  $\sim 17$  in bandwidth, and 110 in pulse duration (in contrast, pulse energy only varies by a factor of  $\sim 2$ ). It is important to note however that the pulse parameters cannot be swept continuously over the totality of such a wide range simply through HWR adjustments. Indeed, as already mentioned, the transition between long- and short-pulse regimes is characterized by abrupt changes in pulse parameters. For example, a 3 ns squared pulse with 5 nm FWHM bandwidth may be turned into a narrow 100 ps pulse with a 40 nm bandwidth during such a transition. Noise-like pulses with parameters included between these two sets of values can still be obtained, however, if the QWR inside the NOLM and the PCs in the ring cavity are properly adjusted as well. The short- (long-) pulse regime can be characterized roughly by pulse durations below (above) 1 ns, and spectral widths above (below) 10 nm.

### 4. Discussion

The mechanism allowing adjusting the temporal and spectral properties of noise-like pulses through HWR adjustments [17]

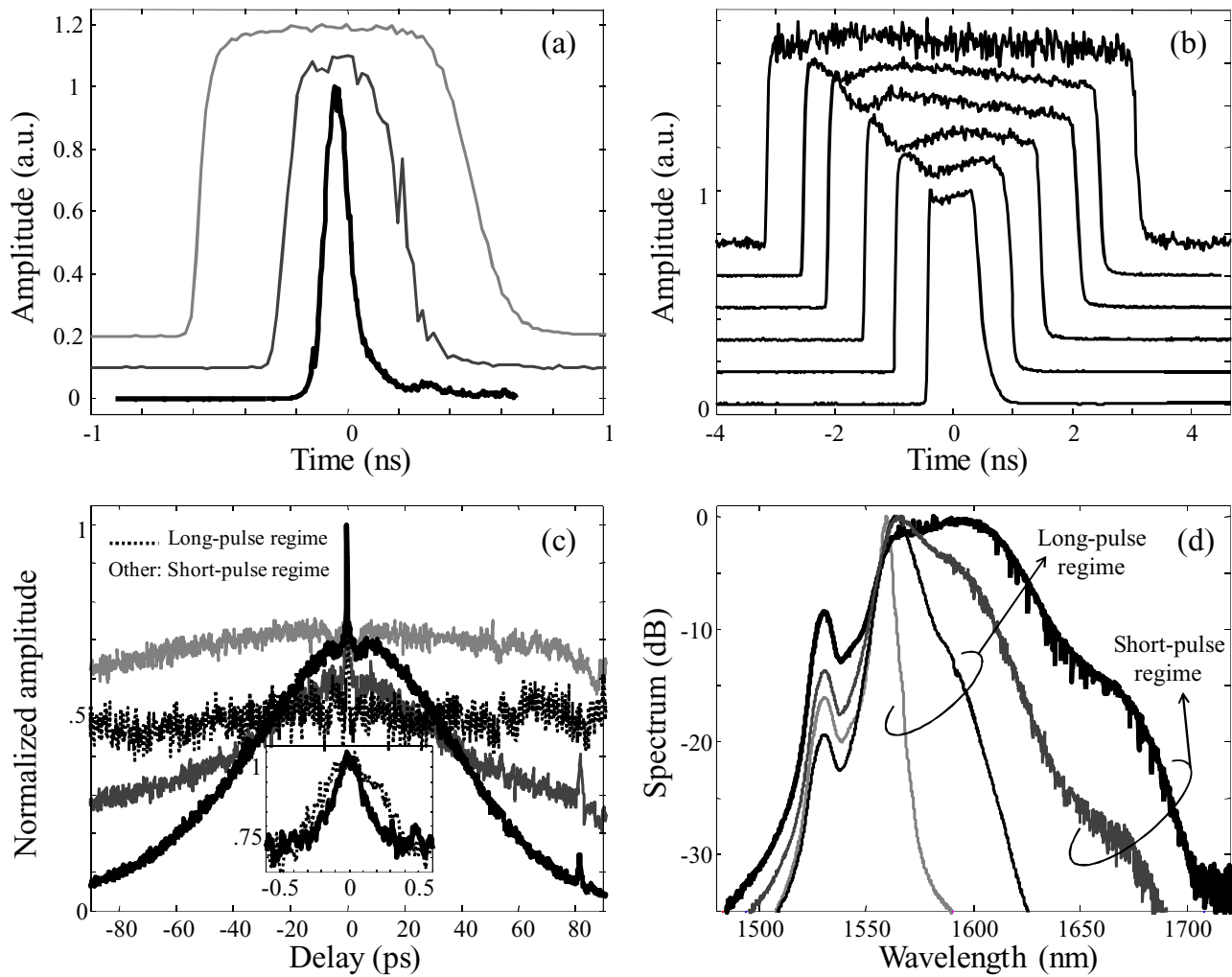


**Figure 3.** Measurements of noise-like pulses for different wave retarder adjustments; (a), (b) time-domain envelopes in the short-pulse (a) and long-pulse (b) regimes measured using a 25 GHz photodetector and a 50 GHz sampling scope (curves were shifted vertically for better viewing); (c) autocorrelation traces (inset shows a close-up on the central spurs for shortest and longest pulses); (d) optical spectra. Assuming a Gaussian envelope, the thick-solid pedestal in figure (c) (80 ps FWHM) allows estimating the shortest pulse duration to  $\sim 57$  ps FWHM (thick solid line in figure (a) is limited by the finite detection bandwidth).

can be summarized as follows. The average peak power of the noise-like pulses tends to adjust itself to the NOLM switching power, as it corresponds to maximal NOLM transmission and thus minimal cavity loss. Hence, as the NOLM switching power is tuned through HWR rotation, the pulse peak power can be increased or decreased over a certain range. At fixed pump power, the pulse energy is roughly constant, so that if peak power increases (decreases), the total pulse duration (and thus the number of sub-pulses in the bunch) decreases (increases). An increase in peak power also causes spectral widening, as a consequence of enhanced Kerr nonlinearity and Raman SFS.

The above mechanism allowed understanding the results of [17], in which noise-like pulses from an anomalous-dispersion cavity could be adjusted over a factor of  $\sim 3$  in both temporal and spectral domains. It also proved useful to interpret part of the results of [23] for a cavity with strong normal net dispersion: when a single noise-like pulse was circulating in the cavity, its duration was adjustable over a factor of  $\sim 4$  and its spectral width over a factor of 3 before this regime was

lost. Focusing now on the results presented here, this mechanism is still valid to explain the pulse adjustability obtained in each regime; however it is insufficient to account for the existence of two distinct regimes, extending very significantly the accessible range of pulse parameters. Hence, further insight into the mechanisms of noise-like pulse formation is required to complete the picture.

A key element to keep in mind for this purpose is the strong dispersion management implemented in figure 1, in which the use of two spans of fibre with large values of dispersion with opposite signs results in a slightly normal net dispersion. In contrast, much less dispersion mapping was used in [17] and [23]. Moreover, we will focus on the variation of the pulse spectrum over one round-trip in each regime. Figure 4 shows the spectra measured at outputs 1 and 2 in the long- and short-pulse regimes. As shown in figure 1, output 1 is inserted in the loop at the end of the DCF section, whereas output 2 is located at the NOLM output (following the standard fibre span). It appears clearly in figure 4 that the two spectra are nearly identical in the long-pulse regime ( $\sim 7$  nm FWHM bandwidth), but



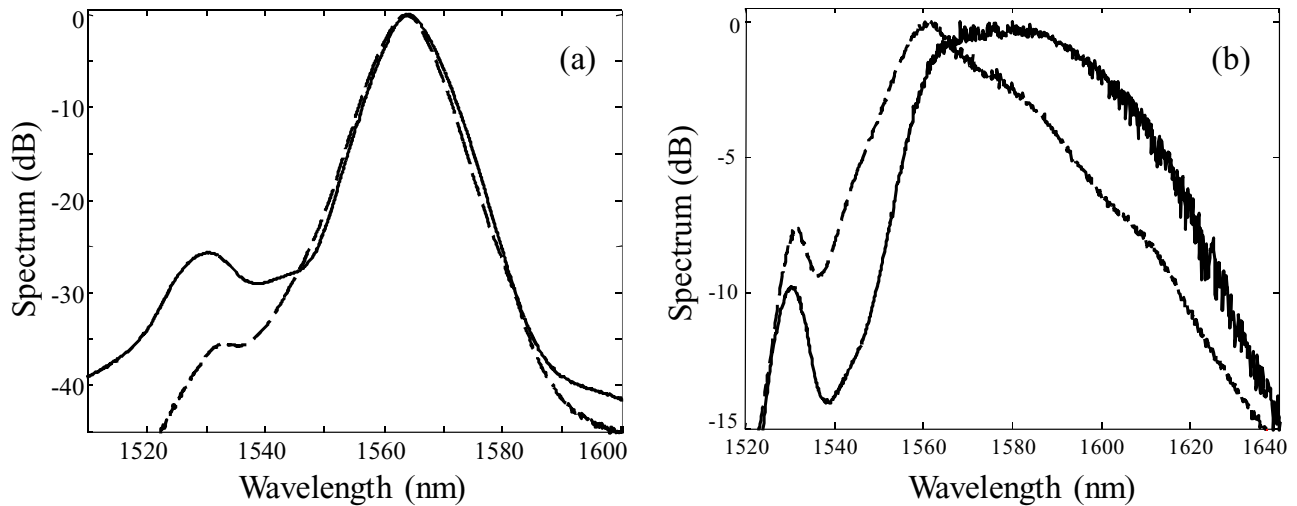


**Figure 4.** Comparison of the optical spectra measured at outputs 1 (dashed) and 2 (solid) in the long-pulse (a) and short-pulse (b) regimes.

are different in the short-pulse regime (the bandwidths are 33 nm and 50 nm at outputs 1 and 2, respectively). Hence we conclude that the spectrum remains nearly constant along the cavity in the long-pulse regime, whereas it varies substantially in the case of short pulses. In contrast, the time-domain pulse envelopes observed at outputs 1 and 2 are undistinguishable in both regimes.

The long pulses observed in this work have the same nature as the noise-like pulses observed in [23], as it appears clearly from their similar rectangular shape, durations of several ns and bandwidth of only a few nm, much narrower than the gain bandwidth. They exemplify the case of normal net dispersion (the absolute value of dispersion is higher in [23]). Because normal dispersion-induced chirp is not able to balance the nonlinear chirp, the pulse duration extends considerably in this regime. This in turn ensures low peak power values, and thus moderate nonlinear effects. Moderate nonlinearities do not strongly broaden the pulse spectrum or cause significant spectral changes along the cavity, not even through the amplifier section due to the much broader gain bandwidth.

In contrast, in the short-pulse regime, peak power is higher, and the Kerr and Raman effects strongly broaden the pulse spectrum. In dispersion-managed systems, because nonlinearities and dispersion interact differently depending on the sign of the latter, the average bandwidth is narrower in the normal dispersion sections and broader in the anomalous dispersion segments [33, 34]. Besides, as the spectrum at the amplifier input becomes broader than the gain bandwidth, each passing through the amplifier causes strong bandpass filtering. These are the two main reasons that explain the strong spectral variations along the cavity, as observed in figure 4(b). Besides, we believe that the NOLM, in the presence of Raman SFS in the loop, also contributes to spectral filtering. In such a situation, the net (or average) dispersion is no longer a good indicator of the *effective* dispersion that prevails in the system. Indeed, because the spectrum is broader in the anomalous dispersion section, this section has a stronger impact on pulse shaping than the normal dispersion section. Hence, even if net dispersion is zero or slightly normal, the effective dispersion can

become anomalous, and be able to balance to some degree the nonlinear chirp [33]. This balance explains why the pulses are much shorter in this regime, with durations of the order of 100 ps. These pulses are comparable to the noise-like pulses observed in [17] in the anomalous dispersion regime, which had durations of a few 100s of ps.

As stated before, a transition from the long- to the short-pulse regime (or conversely) can be readily observed through HWR adjustment. We believe that, when the peak power of the long noise-like pulse is forced to grow due to the increase of the NOLM switching power, at some stage, at least for the highest sub-pulses in the bunch (which in practice appear at the leading edge of the long pulse, see figure 3(b)), nonlinearities become sufficient to cause significant spectral variations along the cavity, thus shifting the effective dispersion to the anomalous regime. These pulses then tend to compact themselves due to the balance between linear and nonlinear chirps, leading to the formation of a short, broadband and high-power noise-like pulse. Conversely, if the short-pulse peak power is forced to decrease through HWR rotation in the opposite direction, at some point the amplitude of spectral variations reduces below the level allowing effective anomalous dispersion to be maintained, and the laser switches back to the long-pulse regime, with a drastic increase in pulse duration and reduction in peak power and bandwidth. A few reports can be found in the literature in which the existence of two noise-like pulsing regimes with different time scales and spectral widths has been observed [13, 18]. As these works deal with dispersion-managed cavities, we believe that the above discussion could be useful to analyze the results of these references.

## 5. Conclusions

In summary, we studied noise-like pulse generation in a strongly dispersion-managed figure-eight laser cavity in the slightly normal net dispersion regime. Mode locking systematically leads to the formation of a single noise-like pulse in the cavity, whose temporal and spectral properties can be

tuned through wave retarder adjustments. In particular, by tuning the angle of a HWR at the input of the polarization-imbalanced NOLM, its switching power can be adjusted, which in turn allows adjusting the pulse duration and spectral width in a versatile way. Wave retarder adjustments also produce a sharp transition between two clearly distinct modes of noise-like pulsing. One of these modes is characterized by a long flat-topped pulse envelope extending over several ns and with a moderate peak power and a narrow and symmetrical spectrum only a few nm wide. The other mode is characterized by sub-ns bell-shaped pulses with higher peak power and a wide, asymmetrical spectrum expanding well beyond the doped fibre gain spectrum on the long wavelength side. The existence of two regimes can be understood by considering the variations of the pulse spectrum along the cavity. In the long-pulse regime, moderate nonlinear spectral broadening and a bandwidth much narrower than the gain spectrum justify that the pulse bandwidth presents little variation over one round-trip. In the normal dispersion regime, nonlinear and dispersion-induced chirps accumulate, leading to the considerable temporal extension of the noise-like pulse. In contrast, in the short-pulse regime, the strong nonlinear spectral broadening, the periodic filtering caused by the limited gain bandwidth and the difference in the interaction between nonlinearity and dispersion in anomalous and normal fibre segments explain that the pulse bandwidth is on average much narrower in the DCF section than in the standard fibre section. As a result, the effective dispersion, in which the dispersion of each segment is weighted by the spectral width of the signal passing through it, is shifted from the slightly normal to the anomalous dispersion regime. In this regime, the nonlinear chirp can partly compensate the linear chirp, so that the pulses are much shorter than in the former regime. By combining the parameter ranges of these two regimes, noise like pulse adjustability over a factor of 110 in duration (57 ps–6.3 ns) and 17 in bandwidth (3.5–59 nm) is demonstrated. We believe that this work could be helpful to understand the complex structure and dynamics of noise-like pulses forming in long fibre lasers.

## Acknowledgement

OP was supported by CONACyT grant 130681.

## References

- [1] Zhang M, Chen L L, Zhou C, Cai Y, Ren L and Zhang Z G 2009 *Laser Phys. Lett.* **6** 657–60
- [2] Yu Z, Wang Y, Zhang X, Dong X, Tian J and Song Y 2014 *Laser Phys.* **24** 015105
- [3] Li X H, Wang Y G, Wang Y S, Zhang Y Z, Wu K, Shum P P, Yu X, Zhang Y and Wang Q J 2013 *Laser Phys. Lett.* **10** 075108
- [4] Matsas V J, Richardson D J, Newson T P and Payne D N 1993 *Opt. Lett.* **18** 358–60
- [5] Duling I N Jr 1991 *Opt. Lett.* **16** 539–41
- [6] Doran N J and Wood D 1988 *Opt. Lett.* **13** 56–8
- [7] Fermann M E, Haberl F and Hofer M 1990 *Opt. Lett.* **15** 752–4
- [8] Tang D Y and Zhao L M 2007 *Opt. Lett.* **32** 41–3
- [9] Ilday F O, Buckley J R, Clark W G and Wise F W 2004 *Phys. Rev. Lett.* **92** 213902
- [10] Kobtsev S M, Kukarin S V, Smirnov S V and Fedotov Y S 2010 *Laser Phys.* **20** 351–6
- [11] Bednyakova A E, Babin S A, Kharenko D S, Podivilov E V, Fedoruk M P, Kalashnikov V L and Apolonski A 2013 *Opt. Express* **21** 20556–64
- [12] Horowitz M, Barad Y and Silberberg Y 1997 *Opt. Lett.* **22** 799–801
- [13] Horowitz M and Silberberg Y 1998 *IEEE Photon. Technol. Lett.* **10** 1389–91
- [14] Kang J U 2000 *Opt. Commun.* **182** 433–6
- [15] Tang D Y, Zhao L M and Zhao B 2005 *Opt. Express* **13** 2289–94
- [16] Zhao L M and Tang D Y 2006 *Appl. Phys. B* **83** 553–7
- [17] Pottiez O, Grajales-Coutiño R, Ibarra Escamilla B, Kuzin E A and Hernandez-Garcia J C 2011 *Appl. Opt.* **50** E24–31
- [18] Vazquez-Zuniga L A and Jeong Y 2012 *IEEE Photon. Technol. Lett.* **24** 1549–51
- [19] Pottiez O, Martinez-Rios A, Monzon-Hernandez D, Salceda-Delgado G, Hernandez-Garcia J C, Ibarra-Escamilla B and Kuzin E A 2013 *Laser Phys.* **23** 035103
- [20] Zhao L M, Tang D Y and Wu J 2007 *Opt. Express* **15** 2145–50
- [21] Kobtsev S, Kukarin S, Smirnov S, Turitsyn S and Latkin A 2009 *Opt. Express* **17** 20707–13
- [22] Zaitsev A K, Lin C H, You Y J, Tsai F H, Wang C L and Pan C L 2013 *Laser Phys. Lett.* **10** 045104
- [23] Pottiez O, Ibarra-Escamilla B, Kuzin E A, Hernandez-Garcia J C, Gonzalez-Garcia A and Duran-Sanchez M 2014 *Laser Phys.* **24** 015103
- [24] Wang Q, Chen T, Zhang B, Heberle A P and Chen K P 2011 *Opt. Lett.* **36** 3750–2
- [25] Wang Q, Chen T, Li M, Zhang B, Lu Y and Chen K P 2013 *Appl. Phys. Lett.* **103** 011103
- [26] Dennis M L, Putnam M A, Kang J U, Tsai T-E, Duling I N Jr and Friebele E J 1997 *Opt. Lett.* **22** 1362–4
- [27] Takushima Y, Yasunaka K, Ozeki Y and Kikuchi K 2005 *Electron. Lett.* **41** 399–400
- [28] Hernandez-Garcia J C, Pottiez O and Estudillo-Ayala J M 2012 *Laser Phys.* **22** 221–6
- [29] Kuzin E A, Korneev N, Haus J W and Ibarra-Escamilla B 2001 *J. Opt. Soc. Am. B* **18** 919–25
- [30] Tanemura T and Kikuchi K 2006 *J. Light. Technol.* **24** 4108–19
- [31] Pottiez O, Kuzin E A, Ibarra-Escamilla B and Mendez-Martinez F 2005 *Opt. Commun.* **254** 152–67
- [32] Ibarra-Escamilla B, Kuzin E A, Zaca-Moran P, Grajales-Coutiño R, Mendez-Martinez F, Pottiez O, Rojas-Laguna R and Haus J W 2005 *Opt. Express* **13** 10760–7
- [33] Nijhof J H B, Forysiak W and Doran N J 1998 *Opt. Lett.* **23** 1674–6
- [34] Grigoryan V S and Menyuk C R 1998 *Opt. Lett.* **23** 609–11